Table 2 Summary of Mössbauer parameters and iron(III)/(II) ratios of fayalites

Locality	Iron(II) peaks			Iron(III) peaks			Ratio of iron(III)/(II) peak areas
	Centre shift	Quadruple splitting	Peak widths	Centre shift	Quadruple splitting	Peak widths	
Rockport, Massachusetts	1.1667	2.8077	0.3442 0.3927				0
Qianan Co., China (ferrifayalite)	1.1687	2.8129	0.4161	0.4312	0.8893	0.4837	1.38
Mourne Mts, Ireland	1.1573	2.8164	0.3386	0.4071	0.8523	0.3877	0.46
Pantelleria, Italy	1.1541	2.8202	0.3872	0.3843	0.9123	0.4360	0.19
St Peter's Dome, Colorado	1.1657	2.8349	0.3885	0.3740	0.6785	0.5543	0.85
Artificial (from slag)	1.1656	2.8240	0.4453 0.4828				0
Dalarne, Sweden	1.1507	2.7910	0.4028 0.4466				0
Varmland, Sweden	1.1694	2.7987	0.2959 0.3597				0
Palmer Peninsula, Antarctica	1.1582	2.8233	0.3231 0.3795				0

Spectra containing four peaks were constrained such that areas and widths of peak pairs were equal, since there was extensive overlap of peaks. This was not necessary for two-peak spectra, and widths of both peaks are given for these. An iron-foil standard was used for all spectra.

Table 3 Microprobe analyses of fayalites of interest to this study

Oxides	Rockport	Qianan	Mourne Mts	Pantelleria	St Peter's Dome
SiO_2	29.06 ± 0.15	30.97 ± 0.67	30.43 ± 0.19	29.72 ± 0.21	29.15 ± 0.39
Al_2O_3	0.00 ± 0.00	0.00 ± 0.00	0.01 ± 0.01	0.00 ± 0.00	0.00 ± 0.00
FeO	67.28 ± 0.33	59.97 ± 0.38	61.86 ± 0.36	63.48 ± 0.21	65.79 ± 0.27
MgO	0.08 ± 0.03	1.45 ± 0.03	0.38 ± 0.02	1.60 ± 0.04	0.00 ± 0.03
MnO	2.28 ± 0.07	0.08 ± 0.04	3.14 ± 0.09	4.08 ± 0.09	4.09 ± 0.13
TiO_2	0.01 ± 0.00	0.00 ± 0.00	0.01 ± 0.01	0.00 ± 0.02	0.00 ± 0.03
CaO	0.00 ± 0.00	0.00 ± 0.00	0.06 ± 0.02	0.51 ± 0.08	0.00 ± 0.00
K_2O	0.00 ± 0.00	0.00 ± 0.00	0.00 ± 0.00	0.00 ± 0.00	0.00 ± 0.00
Total	98.71	96.06	95.89	99.40	99.04

All numbers are in wt %. FeO indicates total iron analysed as FeO.

exchanges more and more of its iron(II) for iron(III), it may at some point distort into the ferrifayalite (laihunite) crystal structure. At this point we would call it ferrifayalite. But chemically, one can still think of these two minerals as forming a solid solution, with fayalite as one endmember and ferrifayalite as the other, even though the crystal structure of the two endmembers is not identical. This classification of iron(III)-rich fayalites may be the most reasonable. It carries with it the implications mentioned for both of the other possibilities.

I thank Professors Roger Burns and Frank Spear for helpful discussions, Professor David Kohlstedt, for TEM work, and the British Museum of Natural History, the Harvard Mineralogical Museum, and the Academica Sinica, for their donation of samples. This work was supported by NSF grant EAR-8016163.

Received 30 December 1982; accepted 21 March 1983.

1. Laihunite Research Group, Guiyang Institute of Geochemistry, Academica Sinica, and 101 Geological Team of Liaoning Metallurgical and Geological Prospecting Company *Geochimica* **6**, 95–103 (1976) (in Chinese).
2. X-Ray Laboratory, Guiyang Institute of Geochemistry, Academica Sinica *Geochimica* **6**, 104–106 (1976) (in Chinese).
3. Laihunite Research Group, Institute of Geochemistry, Academica Sinica, and Geological Team No. 101 of Liaoning Metallurgical and Geological Prospecting Company *Geochemistry* **1**, 105–114 (1982).
4. Ferrifayalite Research Group (Department of Geology of the Peking University, Institute of Geology and Mineral Resources of the Chinese Academy of Geological Sciences) *Acta geol. sinica* **2**, 160–175 (1976) (in Chinese).
5. Nikitin, V. D. *Zap. Vseros. Min. ob-va*, Ser. 2, Ch. 65, 281–288 (1934) (in Russian).
6. Ginzburg, I. V., Lisitsina, G. A., Sadikova, A. T & Sidorenko, G. A. *Akad. Nauk SSR, Trudy Mineralog. Museya* **13**, 16–42 (1962) (in Russian).
7. Deer, W. A., Howie, R. A. & Zussman, J. *Rock-Forming Minerals* Vol. 1 (Longmans, London, 1962).
8. Fu Pingqiu, Kong Youhua & Zhang Liu *Geochimica* **6**, 103–119 (1979) (in Chinese).
9. Fu Pingqiu, Kong Youhua & Zhang Liu *Geochemistry* **1**, 115–133 (1982).

Diagenesis of magnetic minerals in Recent haemipelagic sediments

Robert Karlin & Shaul Levi

School of Oceanography, Oregon State University, Corvallis, Oregon 97331, USA

Rapidly deposited sediments from marine and lake environments are being used increasingly to study decadal to millennial fluctuations in the Earth's magnetic field. The objectives are to gain more fundamental understanding of the geodynamo and to establish a new dating technique for sediments. While lacustrine sections are generally restricted to temperate latitude glacial lakes (≤20,000 yr old), rapidly deposited marine sediments along continental margins potentially offer continuous high resolution, yet long-term records of geomagnetic secular variation. However, to interpret the sedimentary magnetic record accurately, geochemical processes that affect the reliability of the magnetic signal must be understood. We now report downcore magnetic profiles from undisturbed Kasten cores taken in rapidly deposited laminated sediments from the Gulf of California and in bioturbated haemipelagic muds on the Oregon continental slope which give apparently reliable directions, but show dramatic decreases in the intensities of natural (NRM) and artificial (ARM, IRM) remanences with depth.

0028-0836/83/210327—04$01.00

Downcore porewater and solid sulphur analyses show concave-down decreases in porewater sulphate and systematic increases in pyrite and metastable monosulphides. The maximum curvature of the sulphide profile occurs directly below the high magnetization zone. Combined with other compositional and mineralogical analyses, these data suggest that due to oxidative decomposition of organic matter, magnetites and other iron oxides become progressively reduced and subsequently sulphidized and pyritized with depth. Iron reduction seems to occur before sulphide formation. Changes in magnetic stability parameters are consistent with selective dissolution of the finer-sized grains causing downcore coarsening of the magnetic fraction.

The ultimate cause of early diagenesis in marine sediments is the decomposition of organic matter by microbial oxidation. The rates of decomposition and effects on the substrate depend mainly on the availability and reactivity of both organic matter and reductants and the competitive efficiency of microbial populations. Microbes tend to reduce those chemical species which produce the most energy. Thus, in porewaters, reduction tends to occur according to a well defined sequence determined by the free energies of the reactions[1,2]. In the porewaters of suboxic sediments, Froelich *et al.*[3] found a systematic succession of downcore diagenetic reactions proceeding from direct oxidation (by O_2) to manganese reduction, nitrate reduction and ammonia formation. After consumption of labile MnO_2 and NO_3^-, iron oxides are reduced, imparting the characteristic olive grey-green colour to many haemipelagic muds. If sufficient metabolizable organic matter is still present, sulphate reduction begins, followed eventually by fermentation and concomitant methane production. At depths where sulphate is reduced, iron (II) in the porewaters becomes sulphidized, first forming metastable monosulphides (for example, mackinawite) and subsequently pyrite[4–7].

In reducing environments, well crystallized iron oxides have usually been considered to be relatively inert[8]. However, recent recalculations of phase equilibria in the Fe-S-H_2O system[9] suggest that the common ferrimagnetic oxides (magnetite, haematite and maghaemite) may not be thermodynamically stable in the E_h–*p*H conditions found in the porewaters of some anoxic sediments.

Oceanic regimes which are amenable to high-resolution palaeomagnetic studies are those having high terrigeneous sedimentation rates. These areas, generally adjacent to continental margins, also contain large amounts of organic matter, in most cases because of increased fluvially derived terrigeneous carbon input, upwelling-induced high oceanic carbon input, and enhanced preservation due to rapid burial[10]. As a consequence of the high carbon input, direct oxidation (by O_2), if present, is confined to the upper few centimetres of sediment, although this layer generally thickens going offshore[2]. If sufficient organic matter is present, the remainder of the sediment column is anoxic and also sulphidic, because sulphate is abundant in seawater. This two-layer model for haemipelagic sediments contrasts with the deep-sea pelagic 'red' clay regime, where due to low organic input and slow sedimentation, oxidizing conditions can prevail throughout the entire sediment column[11].

We have made a detailed comparative study of the magnetic, geochemical and sedimentological properties of sediments from two contrasting depositional environments, the Gulf of California and the Oregon continental margin. BAM-80-E17 (ϕ27°35.2′ N, λ111°36.6′ W, depth = 625 m) is a 4.5-m Kasten core taken in the Guaymas Basin where the O_2 minimum intersects the slope. The sediments are composed of undisturbed, finely laminated couplets of light coloured diatom-rich ooze alternating with darker organic-terrigenous-diatomaceous muds. Varve chronologies and three ^{14}C dates give sedimentation rates between 140 and 160 cm kyr^{-1}. Major element chemistry shows high correlations ($r > 0.9$) between the terrigenous elements Al, K, Fe and Ti, suggesting downcore mixing of a single terrigenous assemblage, such as from the nearby Rio Yaqui, with Si-rich material, presumably diatoms. This simple model is also supported by X-ray mineralogy and Mössbauer studies.

Downcore magnetic profiles with replicated sampling give stable and apparently reliable directions. The core mean inclination of 41.1° ($\alpha_{95} = 2°$) is comparable to the expected geocentric axial dipole (EGAD) inclination of 46.3°. However, the striking feature of downcore NRM and laboratory-produced anhysteretic (ARM) remanent magnetization profiles, partially demagnetized at 100 Oe a.f. (Fig. 1*a*), is the precipitous decrease in magnetic intensity by over an order of magnitude from the surface to 20–30 cm, whereupon intensities become relatively constant. The stabilities of NRM and ARM, as measured by the median demagnetizing field (MDF), also show a steplike decrease at this depth (Fig. 1*b*).

X-ray powder diffraction patterns of magnetic mineral separates indicate that the top 30 cm consist mainly of pure magnetite ($a_0 = 8.39$Å) with minor amounts of haematite. Ferrimagnetic

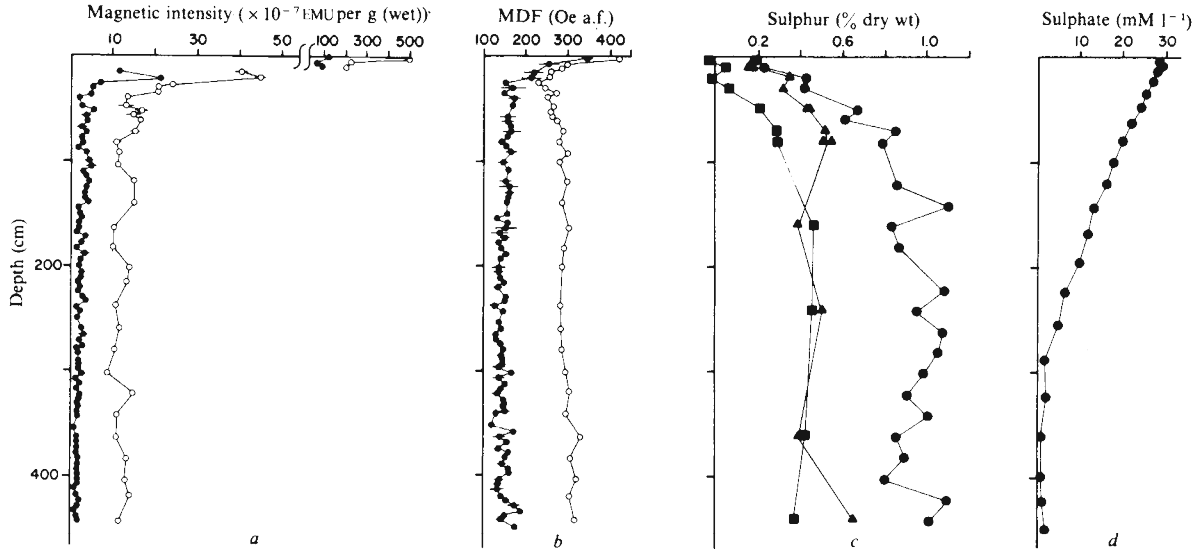

Fig. 1 Downcore magnetic properties and sulphur profiles of Kasten core BAM 80-E17, Guaymas Basin, Gulf of California. *a*, Magnetization intensities, partially demagnetized at 100 Oe a.f.; *b*, median demagnetizing fields of NRM (●) and ARM (○); *c*, sulphate-corrected solid sulphur concentrations of total (●), acid-insoluble (▲) and acid-volatile (■) fractions; *d*, porewater sulphate in mmol l^{-1}. Total sulphur was determined by X-ray fluorescence and LECO analyser; acid-insoluble sulphur was measured by LECO. Acid-volatile is total minus acid-insoluble sulphur, as obtained from LECO.

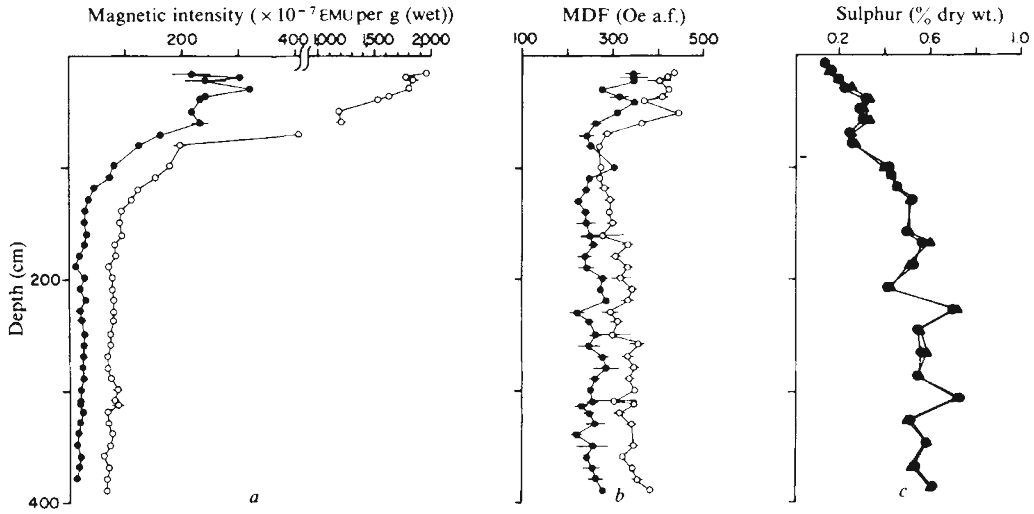

Fig. 2 Downcore magnetic properties and sulphur profiles of Kasten core W7710-28, Oregon continental slope. *a*, Magnetization intensities, partially demagnetized at 150 Oe a.f.; *b*, median demagnetizing fields of NRM (●) and ARM(○); *c*, solid sulphur concentrations of total (●) and acid-insoluble (▲) fractions on a sulphate-free basis, as measured by X-ray fluorescence.

griegite (Fe_3S_4) was not observed. Below 30 cm, the only magnetic species present in the concentrates is pure magnetite. Isothermal remanence acquisition curves[12], as well as the X-ray results and ARM stabilities[13], suggest that the remanence throughout the core is controlled by fine-grained magnetite.

Core W7710-28 is a 3.9-m Kasten core (ϕ44°50.1′ N, λ125°07.5′ W water depth: 1,825 m) taken in a small depositional basin on the lower Oregon continental slope. The sediment consists of heavily bioturbated, mottled to homogeneous olive-green haemipelagic mud. The common red-brown surficial oxic layer was not observed, and a 30 cm boxcore at the same site contained numerous worms, tubules and burrows. Correlation with another ^{14}C-dated core at the same site indicates that the sedimentation rate is ~125 cm kyr^{-1}.

Downcore X-ray determinations and chemical analyses suggest complex mineralogical assemblages which show no coherent variations with sub-bottom depth. Mössbauer studies of bulk material show a remarkable downcore constancy in the chemical properties of the dominant iron-rich species (mainly detrital phyllosilicates).

Magnetic directions are stable and replicable within horizons. The core mean inclination of 62° ($\alpha_{95} = 2°$) closely approximates the EGAD inclination of 63°. However, like the Guaymas Basin sediments, these muds also show a strong downcore decrease in NRM and ARM intensities ('cleaned' at 150 Oe a.f.) and a decrease in MDF with depth (Fig. 2*a*, *b*), with the maximum change occurring between 70 and 100 cm. Magnetic concentrates contain only magnetite ($a_0 = 8.39$Å) throughout the core. The NRM and ARM stabilities (MDFs > 200 Oe) suggest that the magnetite is submicrometre in size[13].

Analyses of sedimentary sulphur in the Guaymas and Oregon sediments (Fig. 1*c*, 2*c*) show an inverse relation between sulphur and magnetic intensity. For the Guaymas sediments, profiles of sulphate-free fractions of total, acid-insoluble in 0.1 M HCl (pyrite + organic sulphur), and acid-volatile (metastable monosulphides) sulphur show systematic increases downcore, reaching relatively constant values at 100–150 cm. The maximum rates of increase occur directly below the zone of high magnetization. In contrast, the porewater sulphate profile (H. Brumsack, personal communication) shows an exponential downcore decrease, indicating sulphate reduction to a depth of ~300 cm (Fig. 1*d*). Downcore sulphur profiles for the Oregon suboxic muds show analogous trends. Acid-insoluble sulphur, presumably in pyrite, and total sulphur increase downcore, reaching relatively constant values at 110–130 cm, directly beneath the zone of high magnetization. An appreciable acid-volatile fraction is not present.

In view of the models of iron and sulphur diagenesis described earlier, these diverse analyses yield a consistent picture of iron diagenesis. In the top 20–30 cm of the anoxic muds of the Guaymas Basin, the iron in fine-grained magnetic oxides (as well as other iron minerals) becomes reduced by reaction with organic matter. Changes in NRM and ARM intensities and stabilities are consistent with selective dissolution of the smaller grains, leading to downcore coarsening of the magnetic fraction.

Iron reduction must occur separately from and before sulphide formation as intermediate metastable sulphides are not produced in the top 20–30 cm, and the various sulphide maxima occur at 50–100 cm, well below the iron reduction zone. This conclusion is in accord with laboratory experiments which have found that iron reduction is independent of sulphate reduction and that nitrate-reducing rather than sulphate-reducing bacteria seem to be responsible for iron reduction[14]. Thus, reduced iron must either diffuse downwards or form an unstable iron (II) oxyhydroxide, silicate or iron-organic chelate which is eventually moved into the zone of sulphidization and pyritization. The iron (II) then reacts with hydrogen sulphide, derived from sulphate reduction, to form mackinawite (FeS) which inverts to pyrite on reaction with elemental sulphur. Because the concentration profiles of the sulphide species are not mirror images of the porewater sulphate profile, the rates of monosulphide formation and pyritization must be controlled by the availability of reactive iron rather than of sulphide.

Similar processes can be recognized in the sub-oxic to anoxic Oregon muds, except that iron reduction and pyritization begins deeper in the sediments, probably as a result of the more oxidizing conditions in the water column and bioturbation in the surficial sediments.

The reduction and dissolution of iron oxides is important to palaeomagnetists studying rapidly deposited sediments in both lacustrine and marine environments. Because iron reduction is not directly coupled to sulphide formation, iron oxides in lake sediments might also undergo reduction with accompanying decreases in remanence and other changes in magnetic properties with depth. Rather than forming sulphides, iron (II) may accumulate to appreciable levels in the porewaters of lakes, eventually reacting to form authigenic minerals, such as siderite ($FeCO_3$) or vivianite ($Fe(PO_4)_2 \cdot 8H_2O$) (ref. 15).

Although iron reduction seems to have little effect on the reliability of palaeomagnetic directions (R.K. and S.L., in preparation), questions arise as to the validity of relative palaeointensity determinations in diagenetically altered sediments. Such estimates rely on the assumptions that the distribution of remanence carriers is uniform throughout the section and that magnetic mineral concentration and field are the only independent variables responsible for the primary remanence[16]. Unless (1) NRM stabilities remain constant downcore, and (2) concentration normalizing parameters (for example, ARM) respond to dissolution-induced grain size changes in an identical manner to NRM, the above assumption(s) will be violated and relative palaeointensity determinations will give erroneous estimates of palaeofield behaviour.

In both oceanic and lacustrine sediments, the extent of iron diagenesis and consequent effects on magnetic properties will depend on the degree to which reducing conditions are established, as well as the initial grain size distribution and crystallinity of the magnetic species. As the redox potential is primarily controlled by the organic matter accumulation rate, the effects of iron reduction will be magnified in regions such as continental borderlands where sedimentation rates are high and the magnetic fraction is fine-grained.

Downcore variations in magnetic properties (such as NRM, ARM, IRM or χ, low field susceptibility) may provide rapid, nondestructive diagnostic tools for geochemists in identifying zones where iron reduction is occurring. In the sedimentary record, where changing climate and oceanic parameters may induce fluctuating redox conditions in the surficial sediments, variations in pyrite concentrations, or conversely, drastic changes in remanence intensity and stability may provide fingerprints of ancient geochemical boundaries. The recognition of these diagenetic processes may become increasingly important as the Deep Sea Drilling Project's Hydraulic Piston Corer provides more long undisturbed sedimentary sections for palaeomagnetic study.

We thank H. Brumsack for providing the porewater sulphate profile; M. Goldhaber for some of the sulphur analyses; C. S. Grommé for use of the USGS cryogenic magnetometer; M. Stuiver for the ^{14}C dates; G. R. Heath, D. Rea and W. Menke for reviews; and E. Suess and H. Schrader for helpful discussion. This work was partly supported by NSF grant OCE 7926440 and a Texaco graduate fellowship to R. K.

Received 20 December 1982; accepted 16 March 1983.

1. Stumm, W. & Morgan, J. J. *Aquatic Chemistry* (Wiley, New York, 1970).
2. Reeburgh, W. S. *A. Rev. Earth planet. Sci.* **11**, (in the press).
3. Froelich, P. N. *et al. Geochim. cosmochim. Acta* **43**, 1075–1090 (1979).
4. Berner, R. A. *J. Geol.* **72**, 293–306 (1964).
5. Rickard, D. T. *Am. J. Sci.* **275**, 636–652 (1975).
6. Goldhaber, M. B. & Kaplan, I. R. in *The Sea* Vol. 5 (ed. Goldberg, E. D.) 569–655 (Wiley, New York, 1974).
7. Berner, R. A. *Early Diagenesis, A Theoretical Approach* (Princeton University Press, 1980).
8. Berner, R. A. *Am. J. Sci.* **268**, 1–23 (1970).
9. Henshaw, P. C. Jr & Merrill, R. T. *Rev. Geophys. Space Phys.* **18**, 483–504 (1980).
10. Heath, G. R., Moore, T. C. & Dauphin, J. P. in *The Fate of Fossil Fuel Carbon Dioxide* (eds Anderson, N. & Malahoff, A.) (Plenum, New York, 1977).
11. Sayles, F. L. & Manheim, F. T. *Geochim. cosmochim. Acta* **39**, 103–128 (1975).
12. Dunlop, D. J. *Geophys. J. R. astr. Soc.* **27**, 37–55 (1972).
13. Levi, S. & Merrill, R. T. *Earth planet. Sci. Lett.* **32**, 171–184 (1976).
14. Sorensen, J. *Appl. envir. Microbiol.* **43**, No. 2, 319–324 (1982).
15. Berner, R. A. *Fortschr. Miner.* **59**, 1, 117–135 (1981).
16. Levi, S. & Banerjee, S. K. *Earth planet. Sci. Lett.* **29**, 219–226 (1976).

A mammal-like reptile from Australia

Richard A. Thulborn

Department of Zoology, University of Queensland, St Lucia, Queensland 4067, Australia

New fossil evidence indicates that a mammal-like reptile inhabited Australia in the early part of the Triassic period (~220 Myr ago). There are no previous reports of mammal-like reptiles from this continent, and the earliest known Australian mammals have been dated as no older than Oligocene (~23 Myr)[1,2]. The evidence is an isolated quadrate bone, recently discovered in Lower Triassic rocks of the Arcadia Formation, south-east Queensland. This bone has morphological peculiarities matched only in dicynodonts (mammal-like reptiles of the infraorder Dicynodontia, order Therapsida) and was probably derived from an animal similar or identical to the common African dicynodont *Kannemeyeria*.

The specimen (Fig. 1*a*, *b*) was collected from freshwater sediments of the Arcadia Formation at a locality known as the Crater, approximately 72 km south-west of Rolleston, south-east Queensland (field locality L78 in Queensland Museum records). The Arcadia Formation (formerly named the Rewan Formation[3]) has already yielded a rich vertebrate fauna[4] including diverse labyrinthodont amphibians[5–8], a thecodontian related to *Chasmatosaurus*[9], an eosuchian similar to *Prolacerta*[10], a paliguanid[10], a procolophonid, a dipnoan, and the subholostean *Saurichthys*[11]. This fauna has affinities with that of the South African *Lystrosaurus* Zone (Lower Triassic) and its equivalents in other Gondwana continents[7,9]. Palynological evidence[12] also supports correlation of the Arcadia Formation with the *Lystrosaurus* Zone.

The newly discovered quadrate is an unusually short, thick and very robust bone, with two strongly developed condyles separated by a deep V-shaped fossa. Its medial condyle is preserved almost intact and is highly distinctive in shape; it resembles part of the rim of a thick wheel, extending through an arc of ~150°. The lateral condyle is damaged but was considerably larger; it seems to have been broadly convex in form (both transversely and longitudinally) and certainly extended a little more ventrally than the medial condyle. The intercondylar fossa is aligned longitudinally, so that the entire articular surface of the quadrate is pulley-like rather than helical. This particular pattern of condyle morphology appears to be unique to dicynodonts[13].

The specimen finds its closest match in the dicynodont *Kannemeyeria*[13–16], being virtually identical to one example illustrated by Watson[13] (Fig. 1*c*, *d*). In view of this extremely close resemblance, the Arcadia quadrate is provisionally identified as that of a dicynodont closely related (or perhaps even identical) to *Kannemeyeria*. The genus *Kannemeyeria* is best known from the Lower Triassic (*Cynognathus* Zone) of South Africa[14,15,17], but has also been reported in the Manda Formation of Tanzania[17,18], the N'tawere Formation of

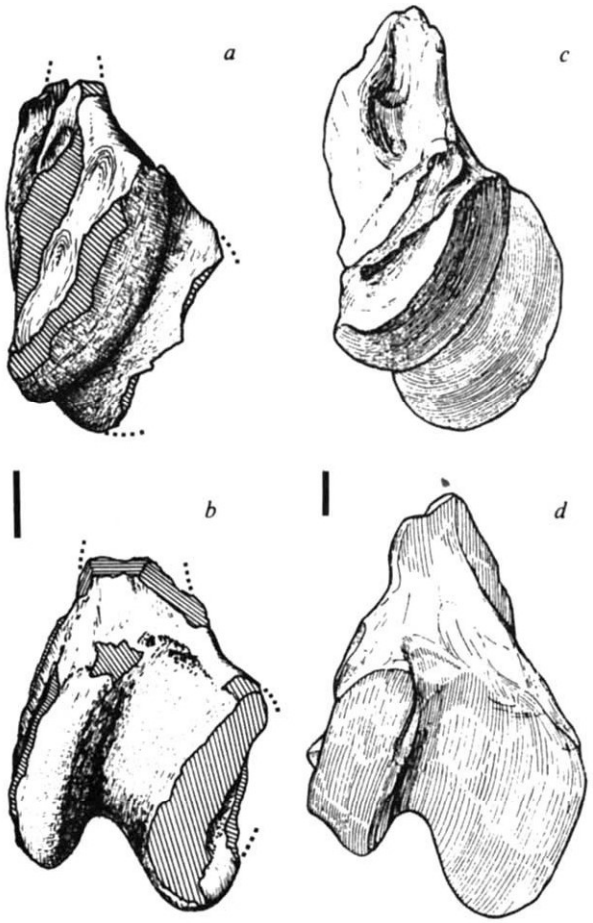

Fig. 1 Left quadrate of dicynodont reptile from the Arcadia Formation, Queensland (*a*, *b*, Queensland Museum F 12178), compared to that of an African specimen of the dicynodont *Kannemeyeria* (*c*, *d*, British Museum (Natural History) R 3763, from Watson[13]). *a* And *c* are medial views; *b* and *d* are anterior views. Scale bars, 1 cm.

0028–0836/83/210330—02$01.00